

# Geochemistry, Geophysics, Geosystems

## RESEARCH ARTICLE

10.1029/2020GC009552

### Key Points:

- Stress loading by the 1996 earthquake (Mw 7.9) on the Minahassa thrust promoted the 2018 Palu earthquake on the Palu-Koro fault
- Stress shadows in the Palu-Koro fault impacted the 2018 Palu earthquake rupture's southward unilateral propagation and termination
- Stress increases in the two seismic gaps to the north and south of the Palu-Koro fault have increased the seismic hazards

### Supporting Information:

Supporting Information may be found in the online version of this article.

### Correspondence to:

C. Liu,  
[changliuu@tongji.edu.cn](mailto:changliuu@tongji.edu.cn);  
[changliuu@gmail.com](mailto:changliuu@gmail.com)

### Citation:

Liu, C., & Shi, Y. (2021). Space-time stress variations on the Palu-Koro fault impacting the 2018 Mw 7.5 Palu earthquake and its seismic hazards. *Geochemistry, Geophysics, Geosystems*, 22, e2020GC009552. <https://doi.org/10.1029/2020GC009552>

Received 14 DEC 2020  
 Accepted 2 MAY 2021

## Space-Time Stress Variations on the Palu-Koro Fault Impacting the 2018 Mw 7.5 Palu Earthquake and Its Seismic Hazards

Chang Liu<sup>1</sup>  and Yaolin Shi<sup>2</sup> 

<sup>1</sup>State Key Laboratory of Marine Geology, Tongji University, Shanghai, China, <sup>2</sup>Key Laboratory of Computational Geodynamics, Chinese Academy of Sciences, Beijing, China

**Abstract** In this study, we calculated the Coulomb stress change before and after the 2018 Palu earthquake (Mw 7.5) induced by historical large earthquakes on and around the Palu-Koro fault (PKF) within Sulawesi Island, Indonesia. We found that the 1996 earthquake (Mw 7.9) on the Minahassa thrust likely promoted the 2018 Palu earthquake by stress loading on its hypocenter. Stress shadows in the PKF impacted the 2018 earthquake rupture's southward unilateral propagation and termination. Stress increases in the two seismic gaps to the north and south ends of the PKF have resulted in increased seismic hazards, calling close attention to hazard prevention in central Sulawesi. This indicates that fault-interaction-induced stress variations on the PKF significantly controlled the 2018 Palu earthquake and its seismic hazards. Our study is important for understanding stress triggering between the subduction earthquakes and intraplate earthquakes in thrust and strike-slip faults systems globally.

**Plain Language Summary** The Mw 7.5 Palu earthquake struck the Palu-Koro fault on September 28, 2018 at Sulawesi Island, Indonesia. The 1996 earthquake (Mw 7.9) on the Minahassa thrust promoted the 2018 Palu earthquake by transferring positive stress at its hypocenter. This earthquake only ruptured the central part (approximately 160 km) on the Palu-Koro fault. Two seismic gaps were created to the north (approximately 180 km offshore) and south (approximately 120 km on shore) of the Palu-Koro fault. The positive stress transferred to these two seismic gaps has increased its seismic hazards. Close attention should be paid to future seismic and consequent tsunami hazard prevention in central Sulawesi.

## 1. Introduction

The Mw 7.5 Palu earthquake struck the Palu-Koro strike slip fault on September 28, 2018 in the Sulawesi Island, Indonesia (Figure 1). This earthquake caused catastrophic disaster to the region of central Sulawesi by claiming over 2,000 lives, affecting more than 53,000 people, and destroying over 68,400 facilities (Song et al., 2019). The Palu-Koro fault was thought to have a high potential of large earthquakes, since it had been quiescent during the past 100 years (Socquet et al., 2019; Stevens et al., 1999; Walpersdorf et al., 1998). Although the Palu-Koro fault is highly likely to produce high-magnitude earthquakes (Socquet et al., 2019), the reasons for the 2018 Mw 7.5 Palu earthquake occurrence have yet to be investigated.

In the first year following the shock, many researchers explored the earthquake rupture process through geodetic and seismic data inversion. The earthquake is suspected to involve predominantly unilateral southward rupture propagation (Bao et al., 2019; Cevikbilen & Taymaz, 2019; Fang et al., 2019; Hayes, 2018a, 2018b; Socquet et al., 2019; Song et al., 2019; Ulrich et al., 2019; Y. Wang et al., 2019). The rupture on the Palu-Koro fault propagated southward for about 130–140 km from the hypocenter. In comparison, northward propagation was observed for only about 20–30 km (Socquet et al., 2019; Song et al., 2019). Significant attention was focused toward the 2018 Palu earthquake rupture's southward unilateral propagation and termination during the past one year. However, the main reasons remain unclear.

The Palu-Koro fault extends around 460 km N-S from the west end of Minahassa trench in the north to the Matano fault in the south. The 2018 Palu earthquake only ruptured the central part (about 160 km) of the Palu-Koro fault (Bao et al., 2019; Cevikbilen & Taymaz, 2019; Fang et al., 2019; Hayes, 2018; Socquet et al., 2019; Song et al., 2019; Ulrich et al., 2019; Y. Wang et al., 2019). Two seismic gaps were left to the north (offshore) and the south (on shore) ends of the Palu-Koro fault with lengths of about 180 and 120 km,

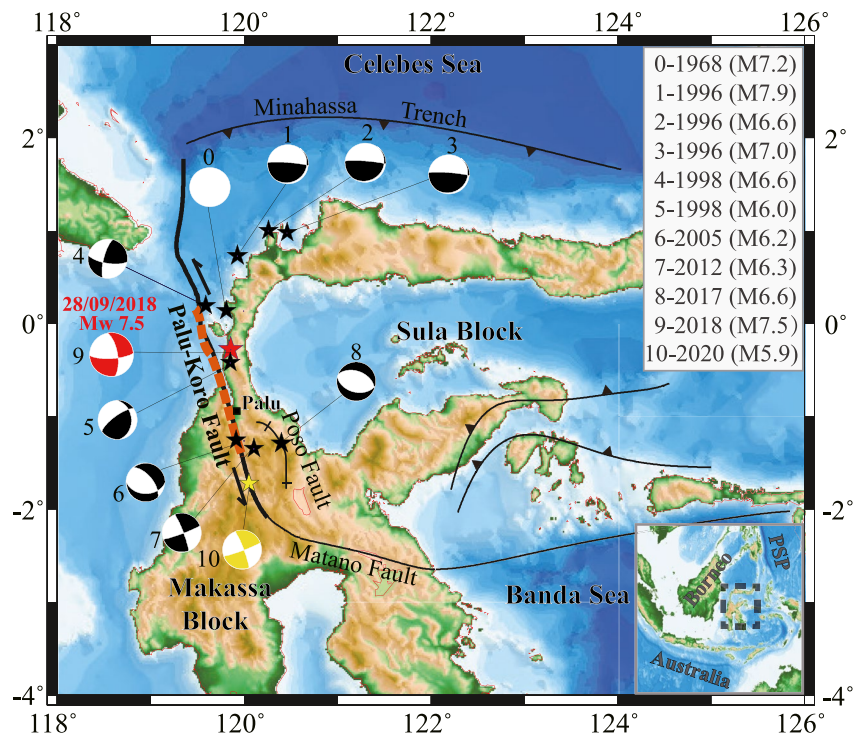


**Figure 1.** Tectonic setting of Sulawesi Island, wherein the black stars show epicenters of the  $M \geq 6.0$  earthquakes spatial distribution on the Palu-Koro fault and the  $M \geq 6.5$  earthquakes around the Palu-Koro fault (distance of  $<200$  km away from 2018 Palu earthquake epicenter); the red star shows the 2018 Palu earthquake epicenter; the yellow star shows the 2020 earthquake epicenter; the beach balls define the historical earthquake focal mechanism (Nos. 1–10); the white solid circle defines the 1968 earthquake with no available focal mechanism (No. 0); and the black lines define the faults. The detailed earthquake parameters (occurrence date, focal depths, and focal mechanisms) are summarized in Table S1 (Supporting Information Text S2). The red dashed line presents the 2018 Palu earthquake rupture. The black rectangle indicates the location of Palu city. The upper right inset shows the date and magnitude of the earthquakes (Nos. 1–10). The lower right inset presents the location of target area in the larger geological setting. PSP = Philippine Sea plate.

respectively (Figure 1). However, the likelihood of imminent seismic gap ruptures remains an open question. As such, it is essential to estimate any future seismic and tsunami hazards within and surrounding central Sulawesi.

The Coulomb stress change ( $\Delta CFS$ ) has been previously suggested to significantly influence seismic activities (Freed, 2005). The importance of stress transfer has been pointed out by studying earthquakes on strike-slip faults (such as the San Andreas fault, North Anatolian, and the Eastern California Shear Zone) (Harris, 1998; Harris & Simpson, 1996; Jaumé & Sykes, 1996; Simpson et al., 1988; R.S. Stein et al., 1994), on normal faults (such as Italy, Greece, and western Turkey) (Harris, 1998; Nostro et al., 1997; R.S. Stein, 1999, 2003), and on continental thrust faults (such as Los Angeles area, Nepal, and eastern Tibet) (Deng & Sykes, 1997; Hardebeck et al., 1998; Harris et al., 1995; Liu et al., 2017, 2018, 2020; Parsons et al., 2008; R.S. Stein et al., 1994; J.C. Wang et al., 2003). However, the stress triggering between subduction earthquakes and intraplate earthquakes, especially in complex thrust and strike slip faults system, and its influence on regional seismic activity has not yet been well studied.

During the past decades, several large earthquakes, such as the 1996 earthquake (Mw 7.9) on the Minahassa subduction zone, were recorded around Sulawesi Island. The occurrence of the 2018 Palu earthquake (Mw 7.5) on the strike slip Palu-Koro fault provides a good opportunity to investigate the fault interaction process between subduction earthquakes and intraplate earthquakes in coupled thrust and strike slip faults systems. To better understand the cause for the 2018 Palu earthquake and the factors impacting its rupture extent, it is necessary to explore the stress state along the Palu-Koro fault by simulating the stress changes caused by regional historical earthquakes.

In order to investigate those questions above, we calculated the  $\Delta$ CFS produced by eight large historical earthquakes ( $M > 6.0$ ) with available focal mechanisms on and nearby the Palu-Koro fault. Stress variations on the Palu-Koro fault prior to 2018 were examined to evaluate any influence on the 2018 Palu earthquake including their impact on the predominantly southward unilateral rupture propagation and termination. We also calculated the  $\Delta$ CFS on the Palu-Koro fault due to the 2018 Palu earthquake. By predicting stress transfer and its evolution by earthquake interaction, we estimate the future hazards in the seismic gaps on the Palu-Koro fault. Our study is important for understanding the reasons for earthquakes occurrence and interaction in central Sulawesi, Indonesia. It is also helpful for understanding stress triggering between subduction earthquakes and intraplate earthquakes in similar systems, globally.

## 2. Geological Setting

Sulawesi is located within central Southeast Asia (Figure 1) where several microplates, specifically, the Indo-Australian, Philippine Sea, and Sunda plates, interact with each other (Hall, 1996). Sulawesi Island moves northwestward following clockwise rotation at a rate of  $4^\circ/\text{Ma}$  about a pole located at the tip of the northern Sulawesi Island. In comparison, the Australian plate drifts northward, the Philippine Sea plate moves westward, and Sunda plate resists in the west (Socquet et al., 2006; Vigny et al., 2002). The Celebes Sea floor subducts southward beneath Sulawesi, and the Minahassa trench accommodates the northwestward movements of the Sula block relative to the Sunda plate (Socquet et al., 2006). The left-lateral strike-slip Palu-Koro fault, which roughly strikes NS, is the main active boundary structure of the western Sula block and has a high long-term slip rate of approximately 40 mm/a. This fault connects the Minahassa subduction zone in the north with the Matano fault in the southeast, running off-shore through the narrow Palu basin. Both the Palu-Koro and Matano faults accommodate the relative motion between the North Sula block and the Makassar block. The Palu-Koro fault has a total length of around 460 km, of which 240 km is off-shore (Watkinson & Hall, 2017). This fault is very important due to its close distance to Palu city with a population of more than 340,000. The 2018 earthquake epicenter was located approximately 75 km north of Palu city, which was heavily damaged by the earthquake triggered tsunami and landslides (Figure 1).

Sulawesi Island is seismically active. However, the Palu-Koro fault exhibited relatively low seismicity levels during the past century (Bellier et al., 2001). Records of historical seismicity in Sulawesi region are poor. Although several damaging earthquakes, such as the 1968 tsunami generating earthquake ( $M 7.2$ ), occurred along and around the Palu-Koro fault (Beaudouin, 1998; Hamilton, 1979; Katili, 1970), the details of these historical earthquakes are rarely known. Since 1968 only eight  $M > 6.0$  earthquakes were recorded with focal mechanisms. These earthquakes are less than 200 km away from the 2018 Palu earthquake epicenter. The present study include three earthquakes ( $M \geq 6.5$ ) (Nos. 1–3) on the Minahassa trench, four earthquakes ( $M \geq 6.0$ ) (Nos. 4–7) earthquakes on the Palu-Koro fault, and one earthquake ( $M \geq 6.5$ ) (No. 8) on the Poso fault (Figure 1). Since the earthquakes of  $M < 6.0$  only induce small stress perturbations in a distance of within several tens of kilometers (Freed et al., 2007), they are excluded from this study.

The present study used a total of nine large earthquakes, including the 2018 Palu earthquake, as the earthquake sources for the calculations. The detailed earthquake source parameters are provided in Table S1 (Text S2) and Figure 1.

## 3. $\Delta$ CFS Variations and Evolution on the Palu-Koro Fault

The combined  $\Delta$ CFS distribution was calculated at 13 km depth (suggested hypocenter depth for the 2018 Palu earthquake) with the receiver faults identical as the focal mechanism (strike =  $350^\circ$ , dip =  $67^\circ$ , rake =  $-17^\circ$ ) of the 2018 Palu earthquake (Hayes, 2018). The computed CFS includes the co-seismic stress and the post-seismic stress change. Viscosity of the mantle can be found in Table S2, and more details of the viscoelastic model can be found in the supporting information.

### 3.1. Stress Change Prior to 2018

Figure 2a shows the cumulative  $\Delta$ CFS map prior to 2018 induced by the three large earthquakes (Nos. 1–3) on the Minahassa thrust. Figure 3a details the induced  $\Delta$ CFS distribution along the Palu-Koro fault. The

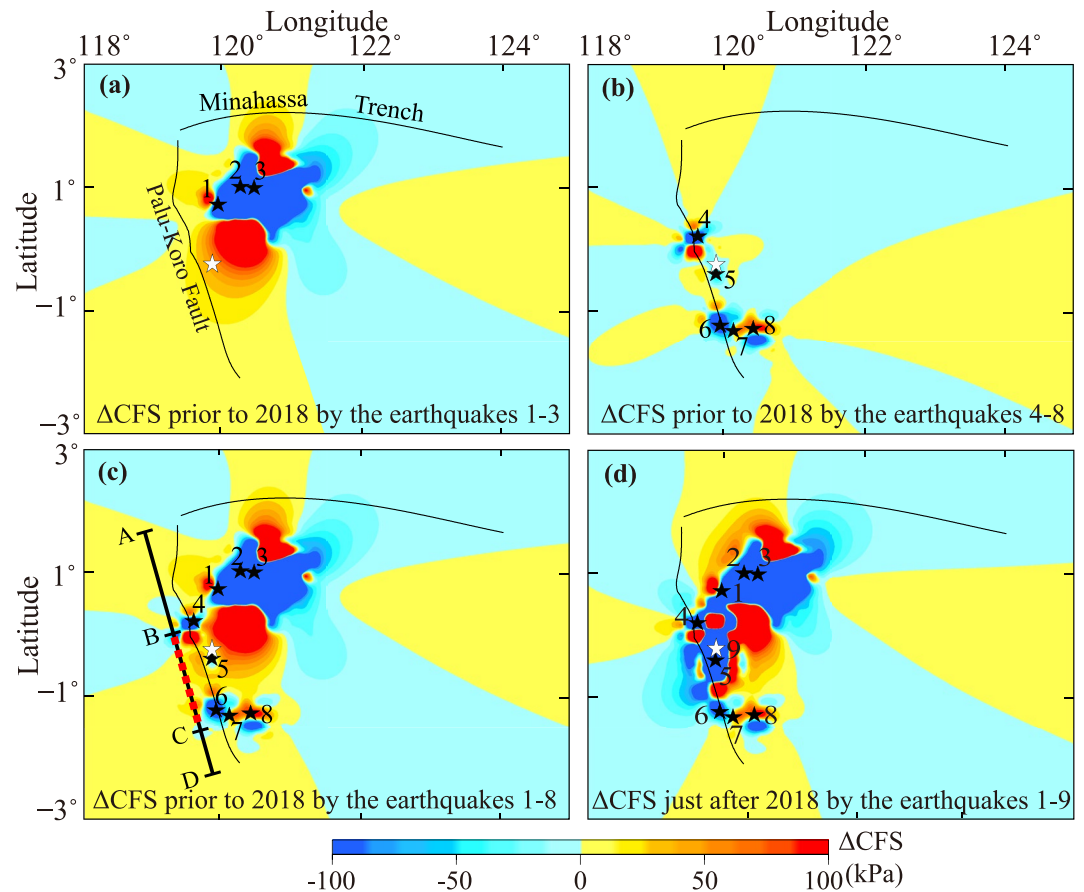


**Figure 2.**  $\Delta$ CFS map at 13 km depth prior to and after 2018. (a) The cumulative  $\Delta$ CFS map following the three earthquakes (Nos. 1–3) on the Minahassa thrust prior to 2018. (b) The cumulative  $\Delta$ CFS map following the five earthquakes (Nos. 4–8) on the Palu-Koro fault and the Poso fault prior to 2018. (c) The cumulative  $\Delta$ CFS map following the eight earthquakes (Nos. 1–8) prior to 2018. (d) The cumulative  $\Delta$ CFS map following the nine earthquakes (Nos. 1–9) just after the 2018 Palu earthquake. The epicenters of the earthquakes (Nos. 1–8) are marked with black stars. The epicenter of the 2018 Palu earthquake (No. 9) is marked by white star.

$\Delta$ CFS was positive over most of the fault, and exhibited an increase of approximately 50 kPa at the 2018 Palu earthquake hypocenter. This stress increase is mainly contributed by the 1996 earthquake (M 7.9) by comparing Figures 3a and s2a to s2c (Text S3).

Figure 2b shows the cumulative  $\Delta$ CFS map prior to 2018 induced by the five large earthquakes (Nos. 4–8) on the Palu-Koro fault and the Poso fault. Figure 3b details the generated  $\Delta$ CFS distribution along the Palu-Koro fault. The  $\Delta$ CFS exhibited a minimal increase of only approximately 1 kPa at the 2018 Palu earthquake hypocenter by the combined effect of these events. However, the  $\Delta$ CFS showed significant decrease near the northern and southern limits of the rupture with the maximum values of  $-300$  kPa and  $-290$  kPa to the north (zone P in Figure 3) and south (zone Q in Figure 3), respectively (Figure 3b). These stress decreases were mainly caused by the 1998 (M 6.6) and 2012 (M 6.3) earthquakes in these two zones (P and Q) on the Palu-Koro fault.

Figure 2c shows the cumulative  $\Delta$ CFS map prior to 2018, which was contributed from the eight large earthquakes (Nos. 1–8). Figure 3c details the induced Palu-Koro fault  $\Delta$ CFS distribution. A combined  $\Delta$ CFS of approximately 51 kPa was observed at the 2018 Palu earthquake hypocenter prior to 2018 induced by the all these historical large earthquakes. The maximum  $\Delta$ CFS drops were about  $-260$  kPa and  $-280$  kPa near the north (zone P) and south (zone Q), respectively, of the 2018 Palu earthquake rupture (Figure 3c).

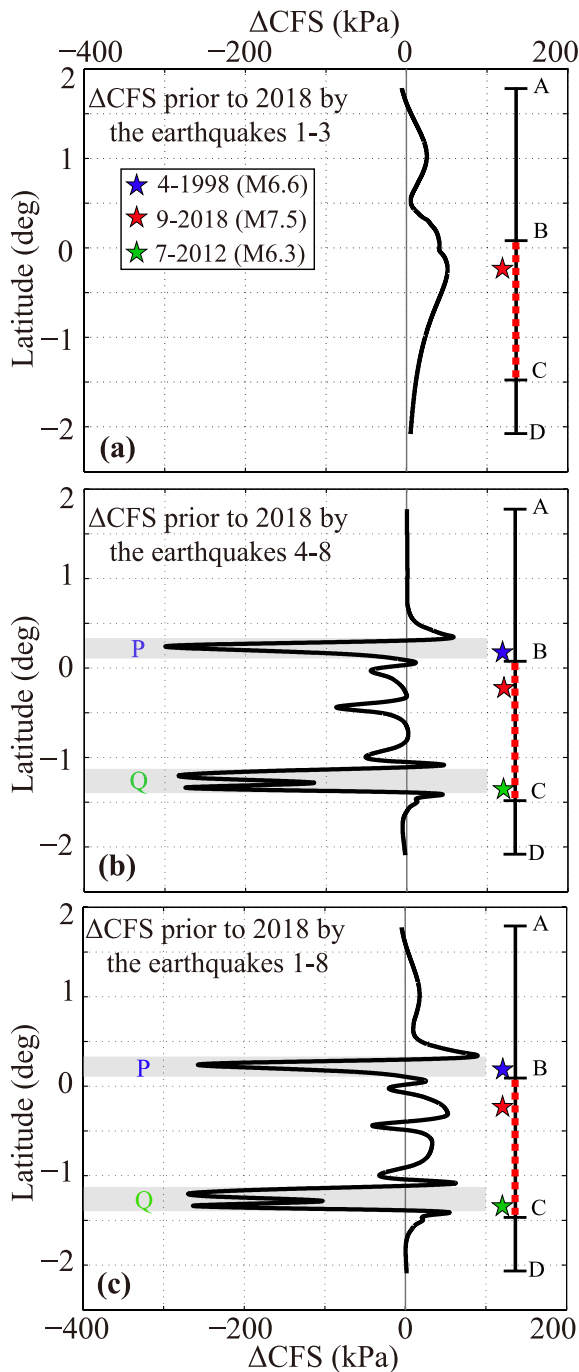


**Figure 3.**  $\Delta$ CFS distribution along the Palu-Koro fault at 13 km depth prior to 2018. (a) The cumulative  $\Delta$ CFS caused by the three earthquakes (Nos. 1–3) on the Minahassa thrust. (b) The cumulative  $\Delta$ CFS caused by the five earthquakes (Nos. 4–8) on the Palu-Koro fault and the Poso fault. (c) The cumulative  $\Delta$ CFS caused by the eight earthquakes (Nos. 1–8) prior to the 2018 Palu earthquake. The blue, red and green stars indicate the latitudes of the 1998 (M 6.6), 2018 Palu (Mw 7.5), and 2012 (M 6.3) earthquakes, respectively. The red dashed line indicates the 2018 Palu earthquake rupture on the Palu-Koro fault. The zones P and Q are marked gray.

### 3.2. Stress Change After 2018

Figure 2d shows the cumulative  $\Delta$ CFS map just after the 2018 Palu earthquake. Figure 4 details the Palu-Koro fault  $\Delta$ CFS distribution at varying depth (5 km, 10 km, 15 km, and 20 km) at time intervals of 0, 20, 50, 100, 200, and 300 years after the 2018 Palu earthquake, assuming no further earthquakes occur. Stress was released in most area between the epicenters of the 1998 (M6.6) and 2012 (M6.3) earthquakes on the Palu-Koro fault just after 2018 (Figure 2d). Two seismic gaps were left to the north (segment AB in Figure 4) and the south (segment CD in Figure 4) ends of the Palu-Koro fault. The  $\Delta$ CFS in these two gaps (segments AB and CD) was increased on average by about 5 and 27 kPa just after the 2018 Palu earthquake, respectively (Figure 4). However, it will be increased to 19 and 56 kPa on average due to viscous relaxation in the mantle over 100 years after the 2018 Palu earthquake (Figure 4) (Table S2).

### 3.3. Inter-Seismic Stressing Rate

The inter-seismic stress accumulation distribution along the entire Palu-Koro fault remains unclear. However, Vigny et al. (2002) calculated the principal horizontal strain rate as approximately 311 and  $-291$  nanostrain/a with the maximum compressional strain axis oriented at  $113^\circ(\pm 2^\circ)$ , using the geodetic data obtained on the Palu-Koro fault in the Palu basin. Given an elastic modulus of  $5.0 \times 10^{10}$  Pa, Poisson's ratio of 0.25, and frictional coefficient of 0.4, Coulomb stress rate on the Palu-Koro fault in the Palu basin was estimated to be approximately 3.6 kPa/a, based on the generalized Hooke's law and the definition of Coulomb stress (Harris, 1998; G.C. King et al., 1994) (see equations [1–6] in the Text S2).

### 3.4. Sensitivity of Stress

The present study also investigated the sensitivity of the stress results to model dependent parameters such as earthquake source parameters, the dip and rake angles, frictional coefficient  $\mu'$ , and mantle viscosity  $\eta$  (Text S4). By considering the uncertainty from all the cases by model parameterization, we found the  $\Delta$ CFS increase was about 34–83 kPa at the 2018 Palu earthquake hypocenter prior to 2018. The maximum  $\Delta$ CFS drops were about  $-212$  to  $-484$  kPa and  $-181$  to  $-473$  kPa near the north (zone P) and south ends (zone Q), respectively, of the 2018 Palu earthquake rupture. The average  $\Delta$ CFS on the two seismic gaps (segments AB and CD) will be promoted to approximately 7–55 kPa and approximately 37–56 kPa, respectively, over 100 years after the 2018 Palu earthquake (Text S4).

## 4. Discussion

### 4.1. Earthquake Triggering

Change of stress field significantly affected the earthquake occurrence and rupture process. The stress evolution in an earthquake cycle in the Palu-Koro fault region was strongly influenced by several major factors, such as inter-seismic tectonic loading and stress perturbation that was induced by historical regional earthquakes. The present study calculated the earthquake stress perturbation by calculating the  $\Delta$ CFS on the

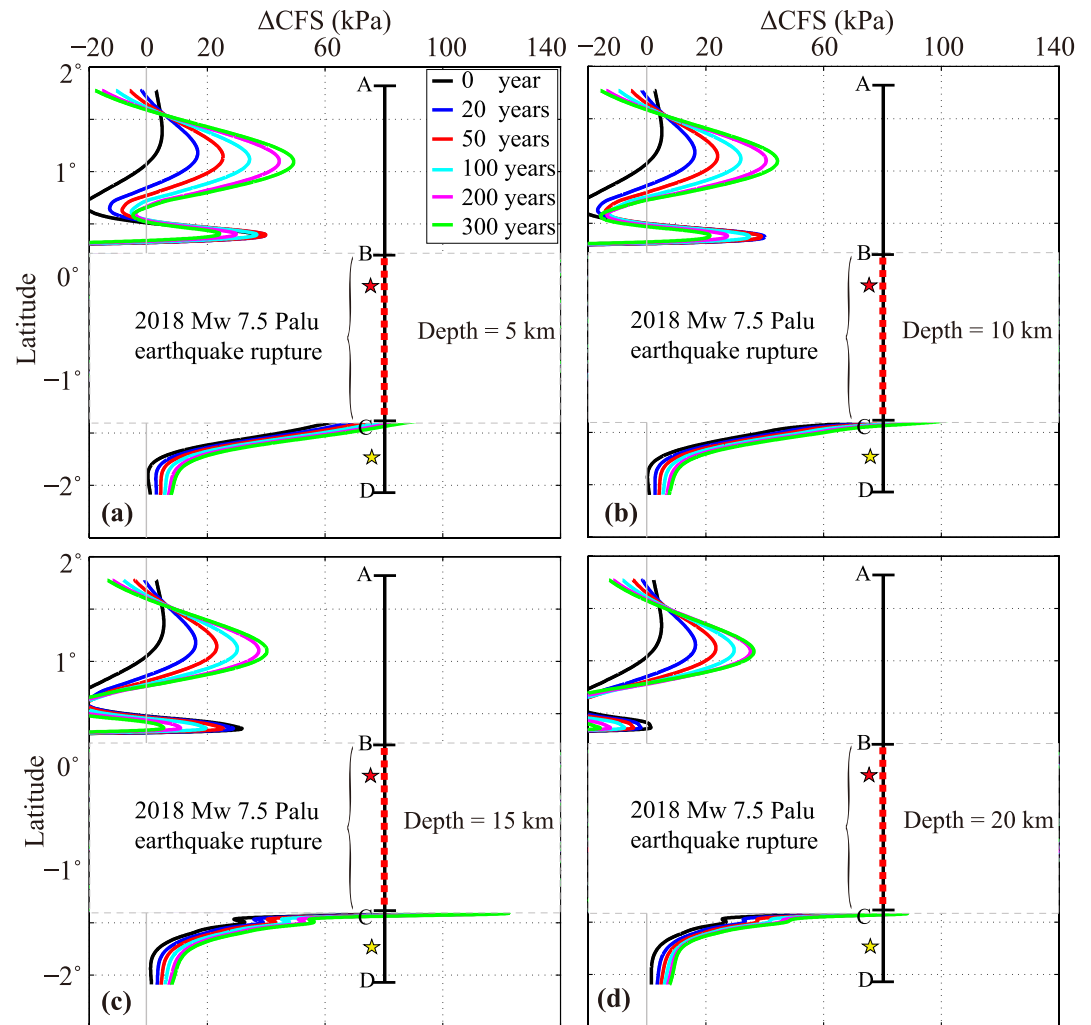


**Figure 4.** Accumulative  $\Delta CFS$  in the two seismic gaps along the Palu-Koro fault at the varying depth of (a) 5 km, (b) 10 km, (c) 15 km, and (d) 20 km induced by the nine earthquakes (Nos. 1–9) at time intervals of 0, 20, 50, 100, 200, and 300 years after the 2018 Palu earthquake. The red and yellow stars indicate the latitudes of the epicenters of the 2018 Palu and 2020 earthquakes on the Palu-Koro fault, respectively. The red dashed line indicates the 2018 Palu earthquake rupture (segment BC) on the Palu-Koro fault. Segments AB and CD indicates the two seismic gaps on the Palu-Koro fault.

Palu-Koro fault prior to the 2018 Palu earthquake, which was contributed from eight large historical earthquakes surrounding the target area across several decades. We then identified the Palu-Koro fault locations that had been loaded or unloaded stress due to fault interaction prior to the 2018 Palu earthquake. As such, complex stress variations along the Palu-Koro fault strike were then observed (Figure 3c).

The  $\Delta CFS$  on the 2018 Palu earthquake hypocenter increased about 51 kPa, which was mainly contributed by the 1996 earthquake (Mw 7.9) on the Minahasaa thrust. In general, a positive  $\Delta CFS$  resulted in an increase in seismic activity in the loaded stress regions. The observed value was much higher than the typical threshold (10 kPa) for triggering earthquakes (Reasenber and Simpson, 1992). As such, the present study hypothesized that the 2018 Palu earthquake was likely promoted by historical earthquakes on the Minahasaa thrust following earthquake triggering theory (Reasenber and Simpson, 1992). Given an inter-seismic tectonic stressing rate of 3.6 kPa/a, the promoted  $\Delta CFS$  (51 kPa) was equivalent to tectonic loading for approximately 14 years.

The Minahasaa thrust and Palu-Koro strike slip fault interaction process is demonstrated by showing the relationship between the inter-seismic crustal displacement due to tectonic loading and earthquake-induced

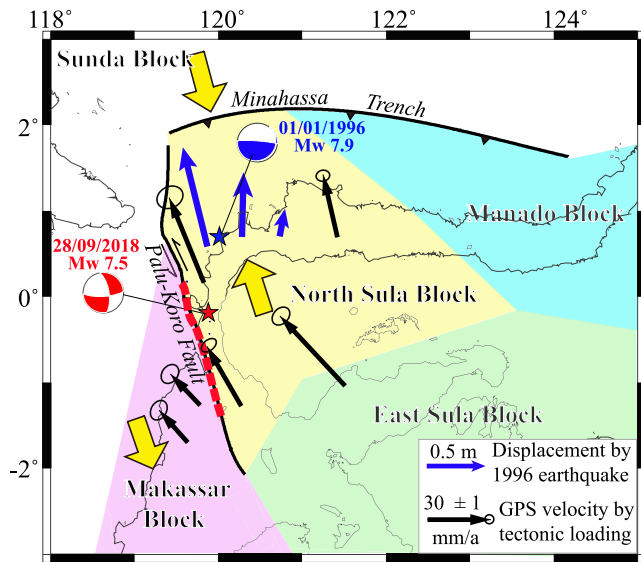


**Figure 5.** Schematic illustration of the interaction between the Palu-Koro fault and the Minahassa thrust by the relative motion of different regional blocks. Blue arrows indicate the crustal displacement induced by the 1996 earthquake (Mw 7.9) on the Minahassa thrust (Gomez et al., 2000). The black arrow indicates the GPS velocity of the crust by tectonic loading (Socquet et al., 2006). The yellow arrow indicates the relative motion of the blocks shown in different colors.

crustal deformation in one map. Figure 5 shows the inter-seismic tectonic loading GPS velocity (Soquet et al., 2006) and the earthquake-induced (1996, Mw 7.9) crustal displacement (Gomez et al., 2000) near the Palu-Koro fault. The inter-seismic tectonic stress loading on the Palu-Koro fault is mainly contributed by the shear between the northwestward moving North Sula block and the southeastward moving Makassar block (Figure 5). Co-seismic displacements derived from GPS data (Vigny et al., 2002) and numerical modeling (Gomez et al., 2000) indicate that the 1996 earthquake (Mw 7.9) led to a northwestward motion of the North Sula block. This earthquake-induced crustal displacement added to the long-term Palu-Koro fault crustal motion (40 mm/a) due to tectonic loading (Figure 5). Consequently, the transferred positive  $\Delta$ CFS on the Palu-Koro fault promoted the 2018 Palu earthquake.

Our finding is congruent with the suggestion of the triggering effect on two 1998 Palu-Koro fault earthquakes (M 6.6 and M 6.3) by the 1996 earthquake (Mw 7.9) on the Minahassa thrust by Vigny et al. (2002). With respect to crustal deformation, this provides new perspectives on fault interaction between the Minahassa thrust and left-lateral strike-slip Palu-Koro faults. This finding is important for a comprehensive understanding the stress triggering in similar faults systems globally. Some other examples are interactions between inland earthquakes (the 1891 M 8.0 Nobi earthquake) in southwest Japan and great interplate earthquakes (the 1944 M 8.0 Nankaido and 1946 M 7.9 Tonankai earthquakes) along the Nankai Trough (F. F. Pollitz & Sacks, 1995; Shikakura et al., 2013; Rydelek & Sacks, 2003).

Vigny et al. (2002) indicated that Palu-Koro fault unclamping due to decreased normal stress by the 1996 earthquake (Mw 7.9) may induce fluid migration into the fault plane of the Palu-Koro fault. The consequent increased pore pressure by the over-pressured fluids in the fault plane might have promoted the two 1998 earthquakes. Details of the pore pressure change were not provided by Vigny et al. (2002). If the pore pressure in the seismogenic depth of the Palu-Koro fault was increased by the 1996 earthquake (Mw 7.9), it might have also impacted the 2018 Palu earthquake to some extent. According to the definition of Coulomb stress (Harris et al., 1998), the pore pressure directly connects to the Coulomb stress on a fault (see equation [1] in the supporting information) by frictional coefficient. Assuming an increase in pore pressure from 10 to 100 kPa and a frictional coefficient of 0.4, the consequent  $\Delta$ CFS increased from 4 to 40 kPa. Based on the stress triggering theory (Reasenber and Simpson, 1992), increasing  $\Delta$ CFS in these values might be important in promoting earthquake failure on the Palu-Koro fault. Future research can be carried out to determine the possible pore pressure change on the Palu-Koro fault caused by historical earthquakes in central Sulawesi.

Note that this study was based on the conventional Coulomb hypothesis that linearly enhances and delays timing of the next earthquake and treats multiple stress steps to straightforwardly sum up, not considering non-linear and time-dependent effect. Many previous studies take the earthquake nucleation process and non-linear process into the triggering effect, which physically explains on-fault and off-fault aftershock sequence responding to the stress change, such as rate and state dependent friction (Cattania et al., 2015; Dieterich, 1994; R. S. Stein et al., 1997; S. Toda et al., 2012), stress corrosion (Scholz, 1990), and time-dependent pore pressure change (Miller et al., 1996). On the other hand, the Omori aftershock law and epidemic type of aftershock sequence also statistically proves earthquake triggering is significantly time-dependent (Felzer et al., 2002; Ogata, 1989). These non-linear space and time dependent triggering studies indicate that the transient effect of stress change would last for the subsequent several decades, particularly in intraplate condition (S. Stein & Liu, 2009; H. Toda & Stein, 2018). Future research could be carried out to explore the non-linear space and time dependent triggering effect on the 2018 Palu earthquake.

#### 4.2. Limitation of the Rupture Extent

We also observed that the  $\Delta$ CFS was decreased by about 260 kPa near the north end of the 2018 Palu earthquake rupture (zone P in Figure 3) by the 1998 earthquake (M 6.6) on the Palu-Koro fault. Generally, a negative  $\Delta$ CFS decreased seismic activities in the regions of the stress shadow. This approach has been used to investigate the role of stress shadow of the 1857 Fort Tejon and 1906 San Francisco earthquakes in the San Andreas Fault (SAF) system, the 1897 Shillong Plateau and 2008 Wenchuan earthquakes following a decrease in the  $\Delta$ CFS (Freed & Lin, 2001; Gahalaut et al., 2011; Harris, 1998; Harris & Simpson, 1996; Liu et al., 2018, 2020; Mallman & Parsons, 2008; Simpson et al., 1988). We proposed that the stress shadow in the zone P (Figure 3) might act as a stress barrier preventing northward earthquake rupture propagation and encouraging its southward propagation.

It should be noted that we did not include the 1968 earthquake in our calculations of the  $\Delta$ CFS due to a lack of reported focal mechanism and earthquake source parameters. The 1968 earthquake epicenter was located to the north of 2018 Palu earthquake. If this event was included in the calculation, we would expect a larger stress release in the stress shadow zone (P) near the north of the 2018 Palu earthquake rupture. Vigny et al. (2002) suggested that the two 1998 earthquakes promoted earthquake inducement in the southern Palu-Koro fault region. According to our results, we suggested that the 1998 earthquake (Mw 6.6) also had a great influence on the seismic activity on the north portion of the Palu-Koro fault by preventing the 2018 Palu earthquake rupture from propagating further northward. The effect of stress shadows on the faults rupture process is not unique for the 2018 Palu earthquake. Previous studies suggested that the stress shadow in the southwest portion of the Longmen Shan fault prohibited the southwestward rupture of the 2018 Mw 7.9 Wenchuan earthquake (Liu et al., 2018). These findings may help characterize earthquake rupture propagation and termination globally, such as the 2002 (Mw 7.9) Denali fault earthquake's unilaterally eastward rupture (Eberhart-Phillips et al., 2003; Liu et al., 2018).

Our results also show that the  $\Delta$ CFS decreased by about 280 kPa near the south end of the 2018 Palu earthquake rupture (zone Q in Figure 3) caused by the 2012 (M 6.3) earthquake on the Palu-Koro fault. Sensitivity test indicated that the  $\Delta$ CFS drops to the ranged of  $-181$  to  $-473$  kPa in the zone Q (Text S4). We believe that the stress drops with these values in the stress shadow zone Q are large enough to terminate the continuing southward propagation of the 2018 Palu earthquake rupture. Our findings are congruent with those of Y. Wang et al. (2019), who calculated the stress change near the south end of the 2018 Palu earthquake rupture caused by the 2005 (M 6.2) and 2012 (M 6.3) earthquakes. However, the magnitudes of stress released by these events were not provided by Y. Wang et al. (2019). By comparing the stress change induced by each event, we found that the stress change of approximately  $-280$  kPa near the south end of the earthquake rupture was mainly caused by the 2012 earthquake (M 6.3). Our findings also support the argument by Wei et al. (2018) that the stress shadow near the south end of the 2018 earthquake rupture might stop further southward earthquake rupture. Wei et al. (2018) also suggested that the stress shadow was likely induced by two earlier historical earthquakes (1907 M 6.3 and 1909 M 7.3 earthquakes), which occurred in the southern segment of the Palu-Koro fault, according to written historical records. However, the earthquake parameters of these two events are not available in the earthquake catalogs of GCMT and USGS. Future research can be carried out to explore the earthquake parameters and stress changes caused by these two events.

It is observed that there are two fault bends with offsets of 4 and 6.5 km to Palu-Koro fault locating to the north and south of the 2018 Palu earthquake rupture, respectively (Bao et al., 2019). One may argue that these fault bends might be restraining and releasing for the 2018 earthquake (Bao et al., 2019), since fault discontinuity or fault bend was suggested to play a major role on the earthquake rupture termination (G. King, 1983; bib\_King\_and\_Nabelek\_1985 G. King & Nabelek, 1985; Wesnousky, 2006, 2008). However, field surveys on coseismic surface ruptures of the 2018 earthquake suggested that the southern termination of the surface rupture was not related to any fault bend and step of the Palu-Koro fault (Wu et al., 2020). Stress shadow revealed by our study gave the reason for the 2018 Palu earthquake rupture termination.

A peak dynamic shear stress at the tip of earthquake rupture front could be large (Lay & Wallace, 1995). Bernardinelli et al. (1999) found that the dynamic Coulomb stress peak value near the fault rupture front is larger than 1.7 MPa during the main subevent rupture of the 1980 Ms 6.9 Irpinia earthquake. It can be expected

that the instantaneous dynamic Coulomb stress increase at the tip of the 2018 Mw 7.5 Palu earthquake rupture front is far over the level of the static stress shadows (of around  $-400$  kPa) revealed in this study. Thus, one may argue that the static stress shadows in this value to the north and south of the fault rupture is not large enough to terminate the 2018 Palu earthquake rupture. This means that the stress shadows might not be the only reason for the 2018 earthquake rupture termination. Some other factors should be playing role in terminating the 2018 Palu earthquake rupture. Schwartz et al. (2012) proposed that paleoseismic history is an important factor to control earthquake rupture termination by investigating the relation between the 2002 Mw 7.9 Denali earthquake rupture and the paleo earthquakes on the eastern Denali fault. Future research should be carried out to explore the possible link between paleoseismic history on the Palu-Koro fault and the 2018 earthquake rupture termination.

#### 4.3. Seismic Hazards After the 2018 Event

After experiencing the five earthquakes (1998 (M 6.6), 1998 (M 6.2), 2005 (M 6.2), 2012 (M 6.3), and 2018 (M 7.5)) on the Palu-Koro fault during the past decades, two seismic gaps were left to the north and the south ends of the Palu-Koro fault. The  $\Delta$ CFS in these gaps (segments AB and CD in Figure 4) was increased on average by about 5 and 25 kPa just after the 2018 Palu earthquake (Figure 4). However, it will be increased to 19 and 56 kPa due to mantle viscous relaxation over the next 100 years after the 2018 Palu earthquake (Text S3). Given an inter-seismic tectonic stressing rate of 3.6 kPa/a, the promoted  $\Delta$ CFS of 19 and 56 kPa was equivalent to tectonic loading for approximately 5 and 16 years in the two gaps. Sensitivity test shows that the value of the  $\Delta$ CFS on segments AB and CD varies in the range of approximately 7–55 kPa and approximately 37–56 kPa (Text S4), respectively, which is higher than the typical stress trigger threshold of 10 kPa (Reasenber and Simpson, 1992). These changes might increase the potential of future seismic hazards in the gaps. This finding helps explain the recent earthquake (Mw 5.9) on March 28, 2020, which occurred in the center of segment CD and 64 km WNW of Pendolo, Indonesia. However, this earthquake was not large enough to fully release the accumulated energy in the segment CD of the Palu-Koro fault. If the whole segments CD (120 km on-shore) or AB (180 km off-shore) rupture, there may be sizable earthquakes of  $M \geq 7.0$  or  $M \geq 7.5$  in each zone, thus releasing accumulated strain at a rate close to 40 mm/yr over the past century (Stevens et al., 1999). Close attention should be paid to the seismic and consequent tsunami hazards prevention in central Sulawesi.

## 5. Conclusions

In order to investigate the reasons for the 2018 Palu earthquake occurrence and the extent of the earthquake rupture, the present study calculated the  $\Delta$ CFS on the Palu-Koro fault following several large historical earthquakes along the Palu-Koro fault with the past few decades. Future seismic hazards on the Palu-Koro fault were also investigated. We reached the following conclusions based on the estimated space-time stress variations on the Palu-Koro fault.

- (1) Fault interactions between the Minahassa thrust and the Palu-Koro fault likely promoted the 2018 Palu earthquake due to loaded stress at the 2018 Palu earthquake hypocenter.
- (2) The 2018 Palu earthquake rupture extent was significantly limited by the stress shadows that were induced by historical earthquakes on the Palu-Koro fault. The stress shadow close to the north of the epicenter of the 2018 Palu earthquake might act as a stress barrier preventing the earthquake northward rupture and encouraging its southward propagation. However, the propagation might be terminated by the stress shadow near the south of the 2018 Palu earthquake rupture.
- (3) Stress increases in the two seismic gaps of the Palu-Koro fault in the north and south ends of the Palu-Koro fault have increased the future seismic and tsunami hazards in central Sulawesi. Close attention should be paid to the seismic and consequent tsunami hazards prevention in central Sulawesi.

## Data Availability Statement

The earthquake data used in this study is available at “zenodo” (<https://zenodo.org/record/3908739#.XvVNutUzYkI>).

**Acknowledgments**

This research was supported by the National Natural Science Foundation of China (No. 41974102), Shanghai Natural Science Foundation (No. 19ZR1459600), the Key Laboratory of Ocean and Marginal Sea Geology, Chinese Academy of Sciences (OMG2019-02), and the National Natural Science Foundation of China (No. U1839207, 41590865). We are very grateful to Jeffrey Freymueller, Mong-Han Huang, Gregory Houseman, and an anonymous reviewer for their constructive comments, which significantly improved the clarity and presentation of the results. We would like to thank the Editor Maureen Long.

**References**

Bao, H., Ampuero, J.-P., Meng, L., Fielding, E. J., Liang, C., Milliner, C. W. D., et al. (2019). Early and persistent supershear rupture of the 2018 magnitude 7.5 Palu earthquake. *Nature Geoscience*, *12*, 200–205. <https://doi.org/10.1038/s41561-018-0297-z>

Beaudouin, T. (1998). Tectonique active et sismotectonique du système de failles décrochantes de Sulawesi Central. Thèse de Doctorat.

Belardinelli, E., Cocco, M., Coutant, O., & Cotton, F. (1999). Redistribution of dynamic stress during coseismic ruptures: Evidence for fault interaction and earthquake triggering. *Journal of Geophysical Research*, *104*(B7), 14925–14945. <https://doi.org/10.1029/1999JB900094>

Bellier, O., Sébrier, M., Beaudouin, T., Villeneuve, M., Braucher, R., Bourles, D., et al. (2001). High slip rate for a low seismicity along the Palu-Koro active fault in central Sulawesi (Indonesia). *Terra Nova*, *13*(6), 463–470. <https://doi.org/10.1046/j.1365-3121.2001.00382.x>

Cevikbilen, S., & Taymaz, T. (2019). Source characteristics of the 28 September 2018 Mw 7.5 Palu-Sulawesi, Indonesia (SE Asia) earthquake based on inversion of teleseismic bodywaves. *Pure and Applied Geophysics*, *176*, 4111–4126.

Deng, J., & Sykes, L. R. (1997). Evolution of the stress field in southern California and triggering of moderate-size earthquakes: A 200-year perspective. *Journal of Geophysical Research*, *102*, 9859–9886. <https://doi.org/10.1029/96jb03897>

Dieterich, J. (1994). A constitutive law for rate of earthquake production and its application to earthquake clustering. *Journal of Geophysical Research*, *99*, 2601–2618. <https://doi.org/10.1029/93jb02581>

Eberhart-Phillips, D., Haeussler, P. J., Freymueller, J. T., Frankel, A. D., Rubin, C. M., Craw, P., et al. (2003). The 2002 Denali fault earthquake, Alaska: A large magnitude, slip-partitioned event. *Science*, *300*(5622), 1113–1118. <https://doi.org/10.1126/science.1082703>

Fang, J., Xu, C., Wen, Y., Wang, S., Xu, G., Zhao, Y., & Yi, L. (2019). The 2018 Mw 7.5 Palu earthquake: A supershear rupture event constrained by InSAR and broadband regional seismograms. *Remote Sensing*, *11*(11), 1330. <https://doi.org/10.3390/rs11111330>

Felzer, K. R., Becker, T. W., Abercrombie, R. E., Ekström, G., & Rice, J. R. (2002). Triggering of the 1999 MW 7.1 Hector Mine earthquake by aftershocks of the 1992 MW 7.3 Landers earthquake. *Journal of Geophysical Research*, *107*, 6. <https://doi.org/10.1029/2001JB000911>

Freed, A. M. (2005). Earthquake triggering by static, dynamic, and postseismic stress transfer. *Annual Review of Earth and Planetary Sciences*, *33*, 335–367. <https://doi.org/10.1146/annurev.earth.33.092203.122505>

Freed, A. M., Ali, S. T., & Bürgmann, R. (2007). Evolution of stress in Southern California for the past 200 years from coseismic, postseismic and interseismic stress changes. *Geophysical Journal International*, *169*(3), 1164–1179. <https://doi.org/10.1111/j.1365-246x.2007.03391.x>

Freed, A. M., & Lin, J. (2001). Delayed triggering of the 1999 Hector Mine earthquake by viscoelastic stress transfer. *Nature*, *411*(6834), 180–183. <https://doi.org/10.1038/35075548>

Gahalaut, V. K., Rajput, S., & Kundu, B. (2011). Low seismicity in the Bhutan Himalaya and the stress shadow of the 1897 Shillong Plateau earthquake. *Physics of the Earth and Planetary Interiors*, *186*(3), 97–102. <https://doi.org/10.1016/j.pepi.2011.04.009>

Gomez, J. M., Madariaga, R., Walpersdorf, A., & Chalard, E. (2000). The 1996 earthquakes in Sulawesi, Indonesia. *Bulletin of the Seismological Society of America*, *90*(3), 739–751. <https://doi.org/10.1785/0119990055>

Hall, R. (1996). Reconstructing Cenozoic SE Asia. In R. Hall, & D. J. Blundell (Eds.), Eds., Tectonic evolution of SE Asia (Vol. 106, pp. 153–184). Geological Society, London, Special Publications. <https://doi.org/10.1144/GSL.SP.1996.106.01.11>

Hardebeck, J. L., Nazareth, J. J., & Hauksson, E. (1998). The static stress change triggering model: Constraints from two southern California after-shocks sequences. *Journal of Geophysical Research*, *103*, 24427–24437. <https://doi.org/10.1029/98jb00573>

Harris, R. A. (1998). Introduction to special section: Stress triggers, stress shadows, and implications for seismic hazard. *Journal of Geophysical Research*, *103*, 24347–24358. <https://doi.org/10.1029/98jb01576>

Harris, R. A., & Simpson, R. W. (1996). In the shadow of 1857—The effect of the Great Ft. Tejon Earthquake on subsequent earthquakes in southern California. *Geophysical Research Letters*, *23*(3), 229–232. <https://doi.org/10.1029/96gl00015>

Harris, R. A., Simpson, R. W., & Reasenber, P. A. (1995). Influence of static stress changes on earthquake locations in southern California. *Nature*, *375*, 221–224. <https://doi.org/10.1038/375221a0>

Hayes (2018a). <https://earthquake.usgs.gov/earthquakes/eventpage/us1000h3p4/finite-fault>

Hayes (2018b). <https://earthquake.usgs.gov/earthquakes/eventpage/us1000h3p4/executive>

Jaumé, S. C., & Sykes, L. R. (1996). Evolution of moderate seismicity in the San Francisco Bay region, 1850 to 1993: Seismicity changes related to the occurrence of large and great earthquakes. *Journal of Geophysical Research: Solid Earth*, *101*(B1), 765–789.

Katili, J. A. (1970). Additional evidence of transcurrent faulting in Sumatra and Sulawesi. *Bandung National Institute of Geology and Mining Bulletin*, *3*, 15–28.

King, G. (1983). The accommodation of large strains in the upper lithosphere of the earth and other solids by self-similar fault systems: The geometrical origin of b-value. *Pure and Applied Geophysics*, *121*, 761–815.

King, G., & Nabelek, J. L. (1985). Role of fault bends in the initiation and termination of earthquake rupture. *Science*, *228*, 984–987.

Lay, T., & Wallace, T. (1995). Modern global seismology. Academic Press.

Liu, C., Dong, P., Zhu, B., & Shi, Y. (2018). Stress shadow on the southwest portion of the Longmen Shan fault impacted the 2008 Wenchuan earthquake rupture. *Journal of Geophysical Research: Solid Earth*, *123*(11), 9963–9981.

Liu, C., Dong, P. Y., & Shi, Y. L. (2017). Stress change from the 2015 Mw 7.8 Gorkhar earthquake and increased hazard in the southern Tibetan Plateau. *Physics of the Earth and Planetary Interiors*, *267*, 1–8.

Liu, C., Zhu, B. J., & Shi, Y. L. (2020). Do the two seismic gaps in the southwest Longmen Shan fault present the same seismic hazards?. *Journal of Geophysical Research: Solid Earth*, *123*. <https://doi.org/10.1029/2019JB018160>

Mallman, E. P., & Parsons, T. (2008). A global search for stress shadows. *Journal of Geophysical Research: Solid Earth*, *113*(B12), 1–16.

Miller, S., Nur, A., & Olgaard, C. (1996). Earthquakes as a coupled shear stress—High pore pressure dynamical system. *Geophysical Research Letters*, *23*(2). <https://doi.org/10.1029/95GL03178>

Nostro, C., Cocco, M., & Belardinelli, M. E. (1997). Static stress changes in extensional regimes: An application to southern Apennines (Italy). *Bulletin of the Seismological Society of America*, *87*(1), 234–248.

Ogata, Y. (1989). Statistical model for standard seismicity and detection of anomalies by residual analysis. *Tectonophysics*, *169*(1–3), 159–174.

Parsons, T., Ji, C., & Kirby, E. (2008). Stress changes from the 2008 Wenchuan earthquake and increased hazard in the Sichuan basin. *Nature*, *454*(7203), 509–510.

Pollitz, F. F., & Sacks, I. S. (1995). Consequences of stress changes following the 1891 Nobi earthquake, Japan. *Bulletin of the Society of America*, *85*, 796–807.

Rydelek, P. A., & Sacks, I. S. (2003). Triggering and inhibition of great Japanese earthquakes: The effect of Nobi 1891 on Tonankai 1944, Nankaido 1946 and Tokai. *Earth and Planetary Science Letters*, *206*, 289–296.

Scholz, C. (1990). Earthquakes as chaos. *Nature*, *348*(6298), 197–198.

- Shikakura, Y., Fukahata, Y., & Hirahara, K. (2013). Long-term changes in the Coulomb failure function on inland active faults in southwest Japan due to east-west compression and interplate earthquakes. *Journal of Geophysical Research: Solid Earth*, *119*(1), 502–518. <https://doi.org/10.1002/2013JB010156>
- Simpson, R., Schulz, S., Dietz, L., & Burford, R. (1988). The response of creeping parts of the San Andreas fault to earthquakes on nearby faults: Two examples. *Pure and Applied Geophysics*, *126*(2–4), 665–685.
- Socquet, A., Hollingsworth, J., Pathier, E., & Bouchon, M. (2019). Evidence of supershear during the 2018 magnitude 7.5 Palu earthquake from space geodesy. *Nature Geoscience*, *12*, 192–199.
- Socquet, A., Simons, W., Vigny, C., McCaffrey, R., Subarya, C., Sarsito, D., & Spakman, W. (2006). Microblock rotations and fault coupling in SE Asia triple junction (Sulawesi, Indonesia) from GPS and earthquake slip vector data. *Journal of Geophysical Research: Solid Earth*, *111*(B8).
- Song, X., Zhang, Y., Shan, X., Liu, Y., Gong, W., & Qu, C. (2019). Geodetic observations of the 2018 Mw 7.5 Sulawesi earthquake and its implications for the kinematics of the Palu fault. *Geophysical Research Letters*, *46*, 4212–4220.
- Stein, R. S. (1999). The role of stress transfer in earthquake occurrence. *Nature*, *402*, 605–609.
- Stein, R. S. (2003). Earthquake conversations. *Scientific American*, *288*(1), 72–79.
- Stein, R. S., Barka, A. A., & Dieterich, J. H. (1997). Progressive failure on the North Anatolian fault since 1939 by earthquake stress triggering. *Geophysical Journal International*, *128*, 594–604.
- Stein, R. S., King, G. C., & Lin, J. (1994). Stress triggering of the 1994 M = 6.7 Northridge, California, earthquake by its predecessors. *Science*, *265*(5177), 1432–1432.
- Stein, S., & Liu, M. (2009). Long aftershock sequences within continents and implications for earthquake hazard assessment. *Nature*, *462*(5). <https://doi.org/10.1038/nature08502>
- Stevens, C., McCaffrey, R., Bock, Y., Genrich, J., Subarya, C., Puntodewo, S. S. O., & Vigny, C. (1999). Rapid rotations about a vertical axis in a collisional setting revealed by the Palu fault, Sulawesi, Indonesia. *Geophysical Research Letters*, *26*(17), 2677–2680.
- Toda, H., & Stein, R. (2018). Why aftershock duration matters for probabilistic seismic hazard assessment. *Bulletin of the Seismological Society of America*. <https://doi.org/10.1785/0120170270>
- Toda, S., Stein, S., Beroza, C., & Marsan, D. (2012). Aftershocks halted by static stress shadows. *Nature Geosciences*, *5*, 410–413. <https://doi.org/10.1038/NGEO1465>
- Ulrich, T., Vater, S., Madden, E. H., Behrens, J., van Dinther, Y., van Zelst, I., & Gabriel, A. A. (2019). Coupled, physics-based modeling reveals earthquake displacements are critical to the 2018 Palu, Sulawesi Tsunami. *Pure and Applied Geophysics*, 1–41.
- Vigny, C., Perfettini, H., Walpersdorf, A., Lemoine, A., Simons, W., van Loon, D., & Bock, Y. (2002). Migration of seismicity and earthquake interactions monitored by GPS in SE Asia triple junction: Sulawesi, Indonesia. *Journal of Geophysical Research: Solid Earth*, *107*(B10).
- Walpersdorf, A., Vigny, C., Subarya, C., & Manurung, P. (1998). Monitoring of the Palu-Koro Fault (Sulawesi) by GPS. *Geophysical Research Letters*, *25*(13), 2313–2316.
- Wang, J. C., Shieh, C. F., & Chang, T. M. (2003). Static stress changes as a triggering mechanism of a shallow earthquake: Case study of the 1999 Chi-Chi (Taiwan) earthquake. *Physics of the Earth and Planetary Interiors*, *135*, 17–25.
- Wang, Y., Feng, W., Chen, K., & Samsonov, S. (2019). Source characteristics of the 28 September 2018 Mw 7.4 Palu, Indonesia, earthquake derived from the advanced land observation satellite 2 data. *Remote Sensing*, *11*(17), 1999.
- Watkinson, I. M., & Hall, R. (2017). Fault systems of the eastern Indonesian triple junction: Evaluation of quaternary activity and implications for seismic hazards. *Geological Society, London, Special Publications*, *441*(1), 71–120.
- Wei, S., Feng, G., Zeng, H., Martin, S., Shi, Q., Muzli, M., et al. (2018). The 2018 Mw 7.5 Palu Earthquake, a Gradually Accelerating Super-Shear Rupture Stopped by Stress Shadows in a Complex Fault System. AGU Fall Meeting Abstracts.
- Wesnousky, S. G. (2006). Predicting the endpoints of earthquake ruptures. *Nature*, *444*, 358–360.
- Wesnousky, S. G. (2008). Displacement and geometrical characteristics of earthquake surface ruptures: Issues and implications for seismic-hazard analysis and the process of earthquake rupture. *Bulletin of the Seismological Society of America*, *98*(4), 1609–1632.

## References From the Supporting Information

- Bassin, C., Laske, G., & Masters, G. (2000). The current limits of resolution for surface wave tomography in North America. *Eos, Transactions American Geophysical Union*, *81*, F897.
- Cattania, C., Hainzl, S., Wang, L., Enescu, B., & Roth, F. (2015). Aftershock triggering by postseismic stresses: A study based on Coulomb rate-and-state models. *Journal of Geophysical Research: Solid Earth*, *120*, 2388–2407. <https://doi.org/10.1002/2014JB011500>
- King, G. C., Stein, R. S., & Lin, J. (1994). Static stress changes and the triggering of earthquakes. *Bulletin of the Seismological Society of America*, *84*(3), 935–953.
- Panet, I., Pollitz, F., Mikhailov, V., Diament, M., Banerjee, P., & Grijalva, K. (2010). Upper mantle rheology from GRACE and GPS postseismic deformation after the 2004 Sumatra-Andaman earthquake. *Geochemistry, Geophysics, Geosystems*, *11*(6).
- Parsons, T., Barka, A., Toda, S., Stein, R. S., & Dieterich, J. H. (2000). Influence of the 17 August 1999 Izmit earthquake on seismic hazards in Istanbul. In *The 1999 Izmit and Duzce earthquakes: Preliminary results* (pp. 295–310). Istanbul.
- Pollitz, F., Banerjee, P., Grijalva, K., Nagarajan, B., & Bürgmann, R. (2008). Effect of 3-D viscoelastic structure on post-seismic relaxation from the 2004 M = 9.2 Sumatra earthquake. *Geophysical Journal International*, *173*(1), 189–204.
- Pollitz, F. F., Bürgmann, R., & Banerjee, P. (2006). Post-seismic relaxation following the great 2004 Sumatra-Andaman earthquake on a compressible self-gravitating Earth. *Geophysical Journal International*, *167*(1), 397–420.
- Wang, G. Q., Ding, G. B., & Yang, J. (2015). *Elasticity*. Tsinghua University Press.
- Wang, R., & Kuempel, H. J. (2003). Poroelasticity: Efficient modeling of strongly coupled, slow deformation processes in a multi-layered half-space. *Geophysics*, *68*(2), 705–717.
- Wang, R., Lorenzo, F., & Roth, F. (2003). Computation of deformation induced by earthquakes in a multi-layered elastic crust-FORTRAN programs EDGRN/EDCMP. *Computers & Geosciences*, *29*, 195–220.
- Wang, S., Xu, C., Xu, W., Yin, Z., Wen, Y., & Jiang, G. (2018). The 2017 Mw 6.6 Poso earthquake: Implications for extrusion tectonics in central Sulawesi. *Seismological Research Letters*, *90*(2A), 649–658.
- Wells, D. L., & Coppersmith, K. J. (1994). New empirical relationships among magnitude, rupture length, rupture width, rupture area, and surface displacement. *Bulletin of the Seismological Society of America*, *84*(4), 974–1002.